



PCCP

**Deformation Mechanisms of Polytetrafluoroethylene at the
Nano and Microscales**

Journal:	<i>Physical Chemistry Chemical Physics</i>
Manuscript ID	CP-ART-08-2018-005111.R1
Article Type:	Paper
Date Submitted by the Author:	12-Nov-2018
Complete List of Authors:	Brownell, Mathew; University of Arkansas, Mechanical Engineering Nair, Arun; University of Arkansas, Mechanical Engineering

SCHOLARONE™
Manuscripts

Deformation Mechanisms of Polytetrafluoroethylene at the Nano and Microscales

Mathew Brownell¹ and Arun K. Nair^{1,2,*}

¹ *Multiscale Materials Modeling Lab, Department of Mechanical Engineering, University of Arkansas, Fayetteville, AR, USA.*

² *Institute for Nanoscience and Engineering, 731 W. Dickson Street, University of Arkansas, Fayetteville AR-72701.*

* *Corresponding author, electronic address: nair@uark.edu; Phone: +479-575-2573, Fax: +479-575-6982*

Abstract

Polytetrafluoroethylene (PTFE) has a low coefficient of friction but also a high wear rate. Numerous studies investigating the possibility of reducing wear and the mechanisms of deformation have been conducted using experimental and computational studies. In this paper the deformation and mechanical failure of single chains, and bulk PTFE are investigated using molecular dynamics (MD). Due to the length scale limitations of the model that MD simulations can investigate, a coarse-grained model is developed and PTFE particles of varying densities are generated to investigate the mechanical properties at the microscale. The coarse-grained potential parameters and coarse-grained model of PTFE are derived from first principle based ReaxFF forcefield simulations and are then used to investigate the microscale mechanical properties of PTFE. The MD study indicate that temperature has a pronounced effect on the maximum strength of a single chain, the elastic modulus is dependent on chain length, and chains shorter than 100 Å have an increase in maximum strength. During indentation and scratch the frictional coefficient of bulk PTFE is dependent on the direction of the scratch on the PTFE substrate. The coarse-grained PTFE simulations show that indentation force is dependent on the density of PTFE, and the smoother the surface roughness of the particle the lower the coefficient of friction. The coarse-grained model that connects the atomic and macroscales of PTFE will lead to direct comparison with experimental PTFE thin films.

Keywords: PTFE deformation, coarse-grained modeling, molecular dynamics, friction

Submitted to Physical Chemistry Chemical Physics

1 Introduction

Polytetrafluoroethylene (PTFE) is used in various fields as sealant material¹, applications in biological implants², and protective surface films and coatings.^{3,4} PTFE has excellent thermal and chemical properties and exhibits hydrophobic behavior.⁵ However, since its discovery in 1938⁶ PTFE has been of great interest for its particularly low coefficient of friction.⁷⁻⁹ Atomic force microscopy reveals that PTFE, once heated, coalesces into a fiber-like cohesive coating.¹⁰ The pulling of the macroscale PTFE orients the fibers in the pulling direction. When tested, the coefficient of friction depends on the direction of the oriented PTFE fibers.¹¹

Despite its unique and useful properties, PTFE has the disadvantage of low wear resistance and loading capacity.^{9,12,13} The longevity of PTFE can be improved by increasing crystallinity, or adding filler particles into the polymer matrix.¹⁴ To improve wear rate, micrometer sized filler particles were introduced into the polymer which increased wear rate by one to two orders of magnitude.^{12,13,15-18} The fillers were also able to increase crystallinity and ultimate strength of the PTFE sample.¹⁹ Nanometer sized particles were also investigated and proven to be effective at reducing wear rate.^{20,21} Copper nanoparticle fillers with a polydopamine coating were found to decrease wear rate even further without increasing the coefficient of friction.^{10,22,23} PTFE particles on the microscale have approximately a spherical shape, but when heated to 372 C°, they form a needle shape.¹⁰ Why the shape changes during heating is unknown and investigating the properties of the shapes of PTFE particles will illuminate failure mechanisms within thin film PTFE.

Investigations involving thin film PTFE and imbedded alumina nanoparticles led to the discovery of the formation of an ultralow wear thin film deposited on a counterface.²⁴ This deposition occurs within the first cycle of sliding on a substrate and creates a robust tribofilm on both sliding surfaces^{3,25,26} which protects and increases wear rate to hundreds of thousands of rubbing cycles.⁴ While some believe the counter-surface effect is purely mechanical²⁷, others have proposed the effects are more structural^{28,29}, or even chemical.⁴ Ultralow wear PTFE composites show exceptional promise for materials of the future.^{20,26,30}

Molecular dynamics simulations have been performed in multiple studies to investigate the effects of filler particles, surface topology, and durability and wear on PTFE at the nanoscale. Studies involving the investigation of the wetting behavior of PTFE³¹, the effects of sliding

orientation of polyethylene³², and the effects of temperature of friction and wear are a few relevant studies conducted using molecular dynamics.³³ Herbold et al. investigated the effects of metallic particles in a PTFE-W-Al composite, they suggested that the filler particles create force chains which help distribute and support any load on the PTFE matrix, increasing its wear resistance and load capacity.³⁴

Multiscale models can be used to increase the length scale under investigation from nanometers to micrometers. Multiscale methods involving PTFE have been studied before to investigate various properties of perfluorosulfonic acid (PFSA) membranes, which consist of PTFE backbone and a perfluorinated ether side chain but never has a coarse-grained model of pure PTFE been investigated for its mechanical properties.³⁵⁻³⁷ The concept of creating a coarse-grained model has been used to investigate the self-folding mechanics of carbon nanotubes³⁸, mechanics of twisting carbon nanotube yarns³⁹, and the aforementioned study investigating PFSA membranes.³⁶

Recent experimental studies show a continuing promise for PTFE as a thin film, particularly with the use of a polydopamine substrate or alumina particles.^{10,22,23,25} Molecular dynamics simulations have been used to investigate the rubbing of PTFE on a metallic substrate as well as PTFE - PTFE interactions.^{4,33} Further improving our understanding of deformation mechanisms on the nanoscale and how those mechanisms affect the microscale particles will allow the design of more durable thin films. In this work, molecular dynamics simulations are used to study solvated, and unsolvated individual PTFE chain response to tensile stress under different temperatures. Indentation and scratch tests are performed on bulk PTFE using MD, and a coarse-grained model of PTFE is developed which increases the length scale of feasible models from nanometers to micrometers. Indentation and scratch tests are then performed on the coarse-grained models that mimic PTFE particles at the macroscale to compare deformation mechanisms between the coarse-grained microscale PTFE and the atomic scale models.

2 Methods

We develop atomistic scale models of individual PTFE chains to study the effect of length and temperature on the chain strength. To study the frictional properties of PTFE particles of varying shape, we develop a coarse-grained model from the atomistic model.

2.1 Atomistic Modeling

Molecular dynamics method is used to simulate tensile tests on single chain PTFE (figure 1A). The chain lengths investigated range from approximately 3 Å to 1000 Å, and only chains longer than 25 Å are studied further due to their stabilized elastic modulus during preliminary testing. 100 Å long chains (figure 1B) are stacked parallel in a square lattice to create a bulk PTFE (figure 1C). Nanoindentation and scratch tests are performed on the bulk PTFE model to study the effect that chain orientation has on the resistance to scratch. All MD simulations are performed using the ReaxFF⁴⁰ force field due to the near quantum mechanical level accuracy⁴¹ and it is especially suited to model fluorinated graphene. The ReaxFF force field is also capable of performing the chemical reactions between PTFE and water molecules. All simulations are performed using Large-scale Atomic/Molecular Massively Parallel Simulator (LAMMPS)⁴² and visualized in Visual Molecular Dynamics (VMD).⁴³

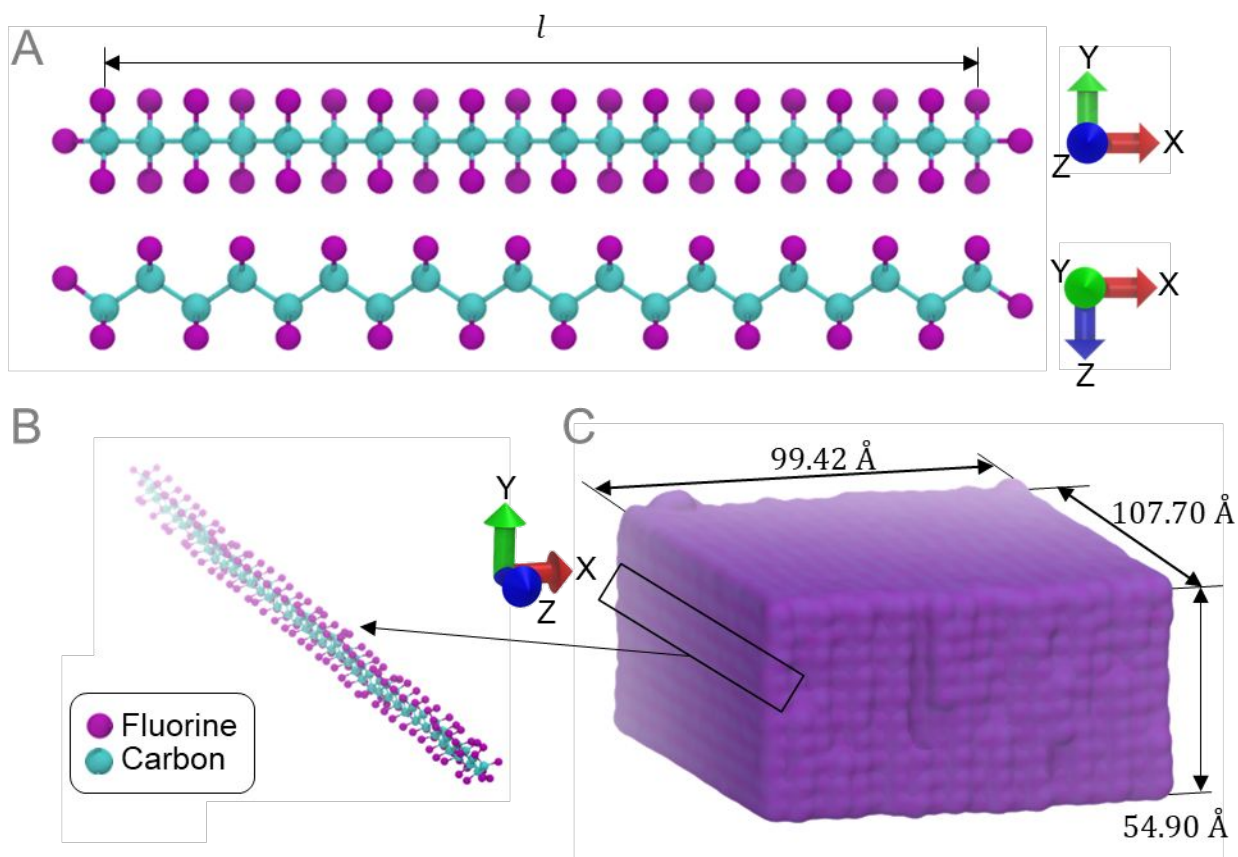


Figure 1 (A) A Single Chain of PTFE comprising of a backbone of carbon atoms bonded to fluorine atoms. (B) Selection of a single PTFE chain used to develop (C) the bulk PTFE model. Each chain was 107.7 Å long after equilibration, placed parallel to the Z axis and approximately 5 Å apart to create the bulk PTFE model.

Understanding atomic scale single chain PTFE and its reaction to stress and strain, temperature, and water will provide insight to nanoscale deformation mechanisms. Measuring the tensile strength of PTFE chains will provide an explanation of failure mechanisms at the nanoscale. Tensile tests are performed on single PTFE chains of varying length, temperature, and water content. Chain lengths (figure 1A) vary from $l = 25, 50, 100, 200, 600$ and 1000 Å, where each chain contains 20, 40, 80, 160, 450, and 755 carbon atoms respectively. Chains are tested at 300 K in 57.5 wt% water and in vacuum. A chain length of 100 Å is chosen to test the effects of temperature and chemical environment. Temperature variation ranged from 300 K to 600 K incremented by 50 K.

In each tensile test simulation, PTFE chains are minimized for 2 ps. To prevent the chain from curling, the carbon atoms at either end of the chain are prevented from moving in the Y and Z direction, restricting their movement parallel to the chain orientation. After equilibration, one end carbon atom is held fixed, while the other is stretched until 20% strain is achieved. This process is carried out for all chain lengths and will determine the tensile strength of individual chain lengths.

To create the bulk PTFE model, chains are oriented in a square lattice, parallel to the Z axis (figure 1B). The PTFE block dimensions are 99 x 55 x 108 Å (figure 1C) after equilibration. The X and Z dimensions are periodic, and the bottom two layers of PTFE chains (10 Å) are held fixed after equilibration is finished, the rest of the atoms are free to move in any dimension while the indentation and scratch tests are performed. To investigate how the chain orientation affects the coefficient of friction, a spherical indenter with radius of 25 Å is indented 10 Å into the surface of the PTFE sample, then scratched at angles 0, 45, and 90 degrees measured from the Z axis, for scratch length of 10 Å.

2.2 Coarse-grained Modeling

Experimental observations show PTFE forms different sized and shaped particles during the annealing process.¹⁰ By developing a coarse-grained force field and model, larger length scales can be achieved than would be possible simply using molecular dynamics. Spanning larger simulation length scale allows for the investigation of micrometer-sized particles as seen in experimental work and how different shapes of these particles change the coefficient of friction.

To develop the coarse-grained force field, multiple PTFE chains are configured to generate a bundle with dimensions 28.18 x 17.75 x 17.41 Å (figure 2A, 2B). Bundle dimensions are chosen to include the twist in PTFE chains (that is inherent to PTFE chain longer than 25 Å) and also considering the ReaxFF force field, which is computationally expensive using molecular dynamics. In this study, PTFE chains are placed in an ideal crystalline alignment. Each bundle is equilibrated at 300 K to allow the bundle to reach a minimum energy and orientation. The relaxed coarse-grained fibers are visually similar to experimentally observed microscale fibers.⁴⁴⁻
⁴⁶ An amorphous phase can lead to change in our coarse-grained parameters especially bending test parameters listed in table 1.

Molecular dynamics is used to perform mechanical tests in order to calculate coarse-grained parameters from fitted energy curves. Three tests are run using the PTFE bundle model, a tensile test, three-point bending test and equilibrium distance test. Each simulation is performed using the ReaxFF force field. The purpose of the tests is to approximate the 1088 atoms in the bundle as three coarse-grained beads (figure 2C, 2D), to increase length scale capabilities by allowing multiple beads to create a fiber (figure 2E). A coarse-grained potential is developed to describe the bond and angle interactions between the three beads, and the interactions of multiple fibers via van der Waals forces. Multiple PTFE beads are used to create a PTFE fiber (figure 2E). Multiple fibers coalesce to form a micrometer sized particle (figure 2F) after equilibration at 300 K.

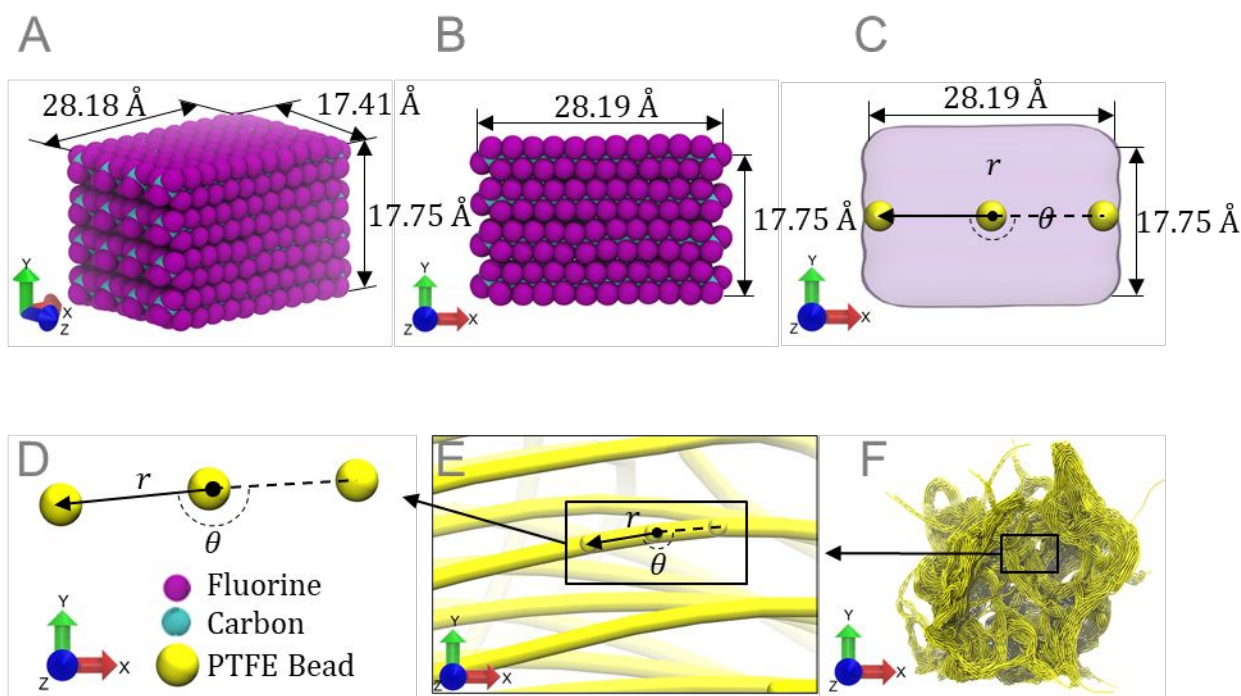


Figure 2 (A) PTFE bundle comprising of parallel PTFE chains. (B) Side view of the PTFE bundle. (C) A silhouette (purple) of figure 2B where three yellow beads are placed showing the scale between molecular dynamics and the coarse-grained beads. (D) Close view of three coarse-grained beads separated by distance r , and forming angle θ , parameters obtained from molecular dynamics bundle simulations. (E) A selection of a PTFE fiber from the coarse-grained model showing the three distinct PTFE Beads. (F) A PTFE particle measuring 0.1 μm across.

The coarse-grained parameters that describe bonding are derived from the energies of the MD simulation of a bundle under tensile stress. During the simulation, the end carbon atoms are held fixed in the Y and Z dimensions to restrict movement of the chain. The fixed carbon atoms are then pulled at a strain rate of 0.05 ps^{-1} until 13% strain. The length and energy of the bundle was recorded for parameter extraction. The strain, and energy of the simulation was plotted and an energy curve was fit to equation 1.

$$E = K_T(r - r_0)^2 \quad (1)$$

The variable r is the length of the bundle, r_0 is the equilibrium length, K_T is the tensile energy constant and E is the energy of the system. The necessary parameters for describing the bonding parameters of the coarse-grained beads are equilibrium length (r_0) and tensile energy constant (K_T). Because three beads are placed in the coarse-grained model to represent the bundle, one bead at each end and one in the middle, the values used in the potential file for the equilibrium bead length (r_0) is 13.60 \AA . The energy constant is then set to $481.07 \text{ Kcal/mol-\AA}^2$, to ensure a correct correlation between the molecular dynamics and coarse-grained simulations.

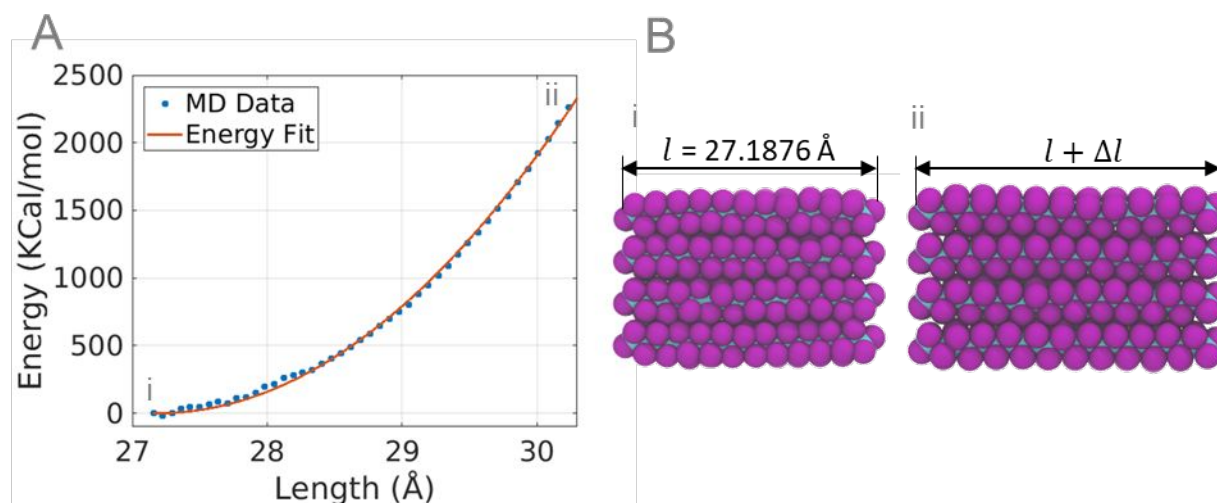


Figure 3 (A) Plot of MD bundle data (blue dots) and the energy fit (red line) used to create coarse-grained model parameters. The energy fit curve is fit to equation 1 and the parameters r_0 and K_T are calculated. (B) Images of PTFE bundle at equilibrium length $l = 27.1876 \text{ \AA}$ (i) and at 11% strain $l + \Delta l = 30.40 \text{ \AA}$ (ii).

A three-point bend test is used to describe the dihedral angles between coarse-grained beads. The end carbon atoms are held fixed in all dimensions, the center carbon atoms were also fixed and displaced in the Y dimension at a strain rate of 0.05 ps^{-1} . The angle of the bundle and the energy are measured and plotted, and an energy curve is fit to equation 2.

$$E = K_B(\theta - \theta_0)^2 \quad (2)$$

The bending energy constant (K_B) and the equilibrium bend angle (θ_0) are used in the coarse-grained potential, while the energy (E) and the bend angle (θ) of the bundle are measured during the simulation.

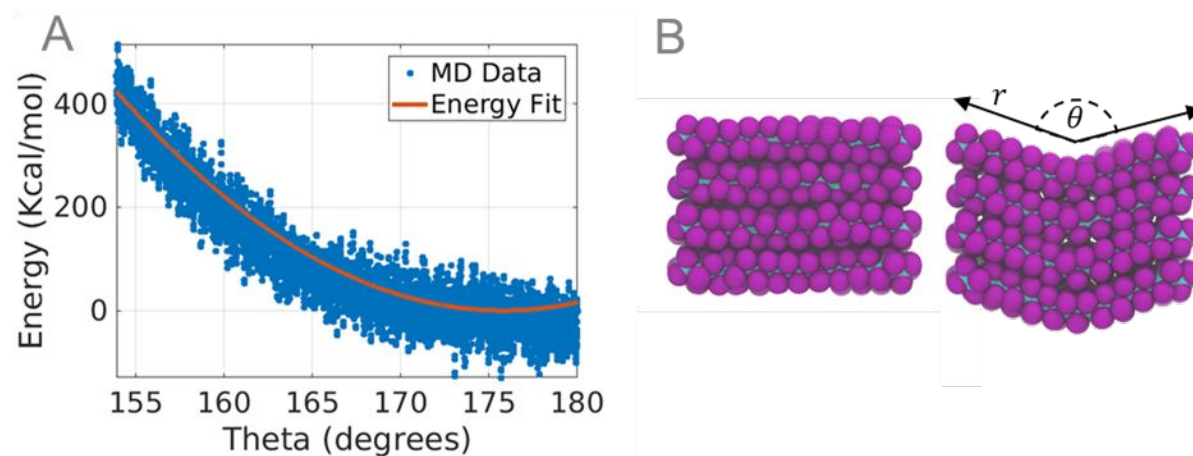


Figure 4 (A) Plot of MD Bundle data (blue) during bending test and the energy fit (red) used to create coarse-grained model parameters. (B) Images of PTFE bundle before and during the bending test.

The van der Waals interactions in the coarse-grained model are determined by the attractive or repulsive forces from the MD simulations. The equilibrium test uses two separate completely fixed bundles parallel to one another, which are brought closer together as the simulation progresses. The distance and energy of the system is measured and plotted, and an energy curve is fit to the potential energy of the two bundles using the Lennard-Jones 12:6 curve (equation 3).

$$E = 4\epsilon \left[\left(\frac{\sigma}{r} \right)^{12} - \left(\frac{\sigma}{r} \right)^6 \right] \quad (3)$$

The energy well depth at equilibrium (ϵ), and the distance parameter (σ) are calculated via the curve fit. The distance between PTFE bundles (r) and the energy (E) of the bundle are measured

during the simulation. The parameters necessary to model the coarse-grained force field are the energy well depth at equilibrium (ϵ), and the distance parameter (σ).

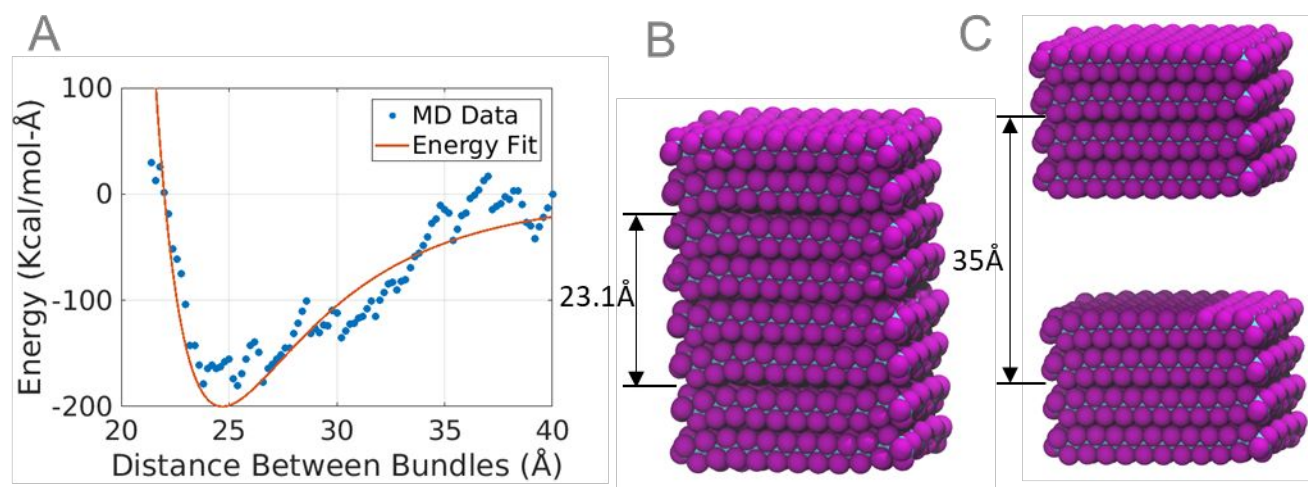


Figure 5 (A) Plot comparing two molecular dynamics equilibrium distance data points to the Lennard Jones curve. Images show the bundle at distances of 23.1 Å (B) and 35 Å (C).

The parameters gathered from the equilibrium distance test are those that create the best Lennard Jones fit to the data. The energy cutoff distance r_{cut} was chosen to be 45.65 Å, when the energy of two interacting bundles was zero. The values for the energy well depth, and the zero-crossing distance were chosen to ensure the equilibrium distance and the equilibrium energy matched the bundle simulation. Due to the thermal fluctuations in the data used to fit the Lennard Jones curve, the coarse-grained force field may cause variation in the forces predicted. By conducting parametric studies, we have quantified the variation in forces to be up to 5 nN. The necessary parameters to model PTFE are summarized in table 1.

Table 1. List of Coarse-grained Parameters			
Simulation	Parameter Description	Value	Units
Tensile Test	Energy Parameter (K_T)	481.07	$\frac{Kcal}{mol \text{ \AA}^2}$
	Equilibrium Bond Distance (r_0)	13.60	\AA
Three Point Bend Test	Energy Parameter (K_B)	1330.82	$\frac{Kcal}{mol rad^2}$
	Equilibrium Angle (θ_0)	177.31	Degrees
Equilibrium Distance Test	Energy Well Depth (ϵ)	30.60	$\frac{Kcal}{mol}$
	Zero-crossing Distance (σ)	23	\AA
	Energy Cutoff (r_{cut})	50	\AA

Table 1 The list of parameters extracted from the molecular dynamics simulations on PTFE bundles. Three tests are performed: tensile, three point bend, and equilibrium distance tests. These parameters are used to define the bonding, angle, and van der Waals forces between PTFE beads in the coarse-grained potential.

A three-bead model is generated to test the coarse-grained parameters against the bundle simulations. Tensile, three point bend, and equilibrium distance tests are performed using the new coarse-grained model and potential. Results from the coarse-grained simulations recreate the MD simulation energies in the coarse-grained potential.

Using the coarse-grained equilibrium distances, PTFE beads are placed into 10,000 PTFE fibers. To create the model, 500 \AA long fibers are positioned and oriented randomly. The model was set to equilibrate at 300 K for 15.6 ns. The PTFE fibers coalesce into a porous interwoven mesh which gradually condense to a particle.

The resultant nanoparticle with an approximate spherical shape is referred here as the porous nanoparticle (Porous) (figure 6A&B). A flattened particle (figure 6C&D) with lower porosity (Flat) was also generated using LAMMPS which is half the original height of the porous nanoparticle. Finally, a high density needle shaped (Needle) particle (figure 6E&F) was also

generated with a similar length to width ratio (3.26) as fibers found in experimental works (2.6-3.77).¹⁰ The radial distribution of atoms in each model is measured and indicates that the models are indeed different sizes and shapes of the same material with different densities (figure 6F). Various shapes of PTFE particles are observed in experimental literature and our particles were modeled after the shape and size of these particles.^{10,47} In our studies the porous model replicates the particles observed in experiments at room temperatures before annealing. We compress the porous model to different densities to generate the flat and needle particle models. The density of the porous, flat, and needle model are 0.7376, 0.8420 and 1.0120 g/cm³ respectively which are similar to the density of PTFE powder ranging from 0.5 to 2.0 g/cm³.⁴⁷

Fibers of equilibrated coarse-grained models were measured ~ 10 nm in diameter. AFM images from experimental studies show PTFE fibers ranging from 400 nm to 10 nm in diameter and forming an entangled web-like structure, which is also observed in the equilibrated coarse-grained particles.^{46,48} Although bundle simulations use an ideal structure of PTFE to approximate the coarse-grained parameters, the coarse-grained particles contain a similar density and shape to particles observed experimentally.^{10,47}

Indentation is performed at the same location for all particles. A purely repulsive spherical LAMMPS indenter with a diameter of 50 nm is used to indent each nanoparticle. The indentation speed was held constant at 5 m/s for each indenter, and an indentation depth of 10 nm was studied.

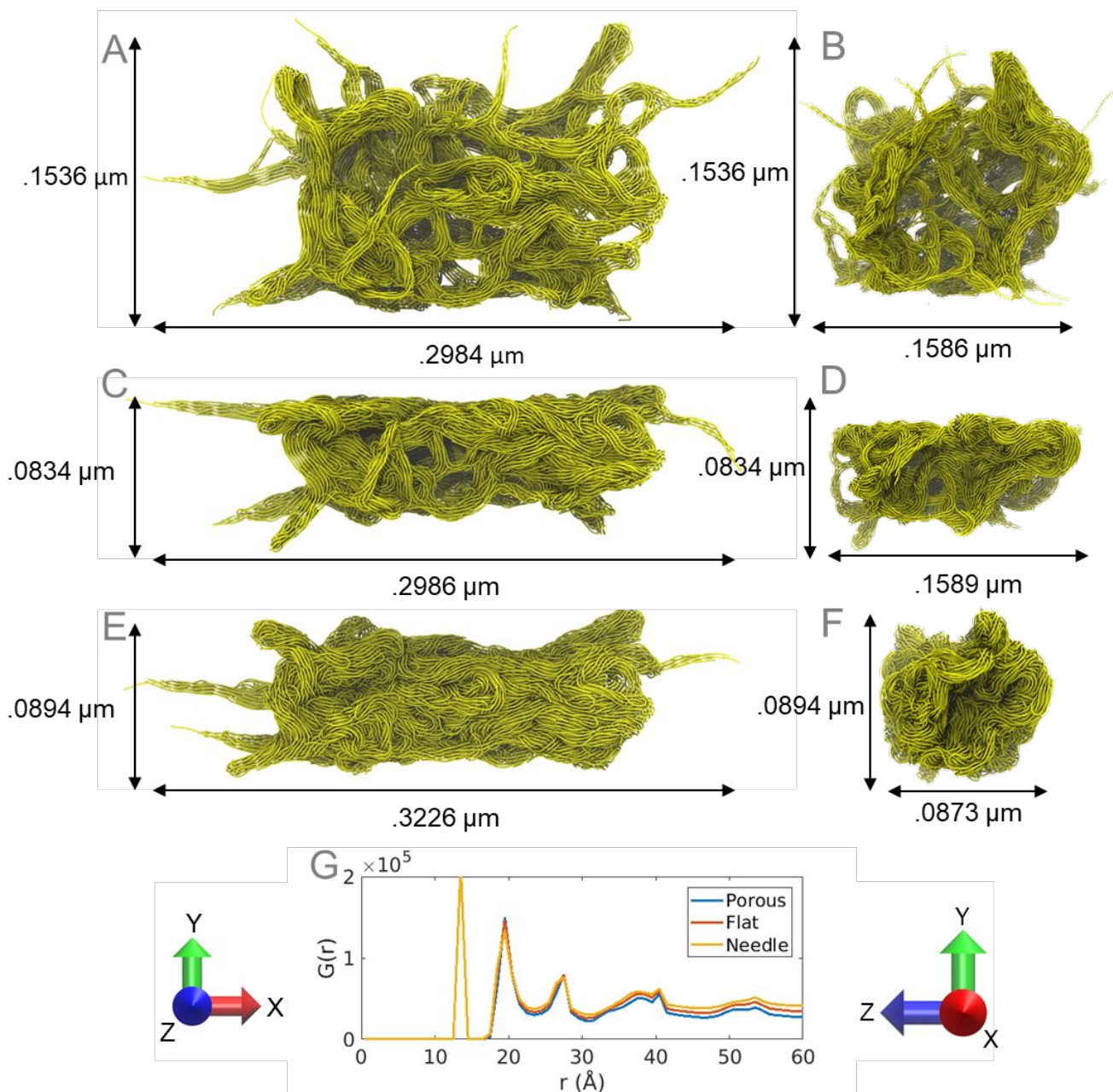


Figure 6 (A) The porous particle (Porous) is generated by equilibrating random PTFE fibers for 15.6 nanoseconds. (B) Side view of porous particle. (C) The flattened particle (Flat) is generated by indenting the porous particle in the Y dimension until the particle is half the original size. (D) Side view of flattened particle. (E) We generate the needle particle (Needle) by varying the density of the PTFE fibers. (F) Side view of needle particle. (G) Radial distribution function showing that each particle contains the proper peaks where PTFE coarse-grained beads rest, but each has a difference in density.

3 Results and Discussion

3.1 Single Chain PTFE Simulations

Molecular dynamics simulations on single PTFE chains study how the initial chain length affects the maximum tensile stress before the chain fails. The chains are studied in vacuum and in a water environment, at 300 K. Results from the length studies shows the chains shorter than 100 Å withstand a slightly higher stress than the others, for this reason the 100 Å long chain was selected for the temperature study. The pulling velocity is investigated and found to have a negligible effect on the mechanical properties of atomistic PTFE chains.

3.1.1 Elastic Modulus

To explore the effects of chain length on elastic modulus, and also to compare results with previous studies, the length of chains investigated ranged from 3 Å to 1000 Å. Values for elastic modulus of PTFE have been reported at 160 GPa using force field calculations and 221 and 247 GPa using DFT.⁴⁹⁻⁵¹ In order to compare our MD model results to density functional theory (DFT) calculations. We use the smallest chain of PTFE to recreate the simulation conditions of DFT; the elastic modulus at 1 K is calculated to be 248.1 GPa agreeing with previously reported data. We observed an increase in the elastic modulus of the PTFE chains as the chain length increases at 300 K (figure 7A). Using the linear elastic region (from 0 to 2.5 % strain) of the stress strain curve (see figure 8A and B), the elastic modulus is calculated to be 525 GPa for the 100 Å chain at 300 K in vacuum and 524.8 GPa in water.

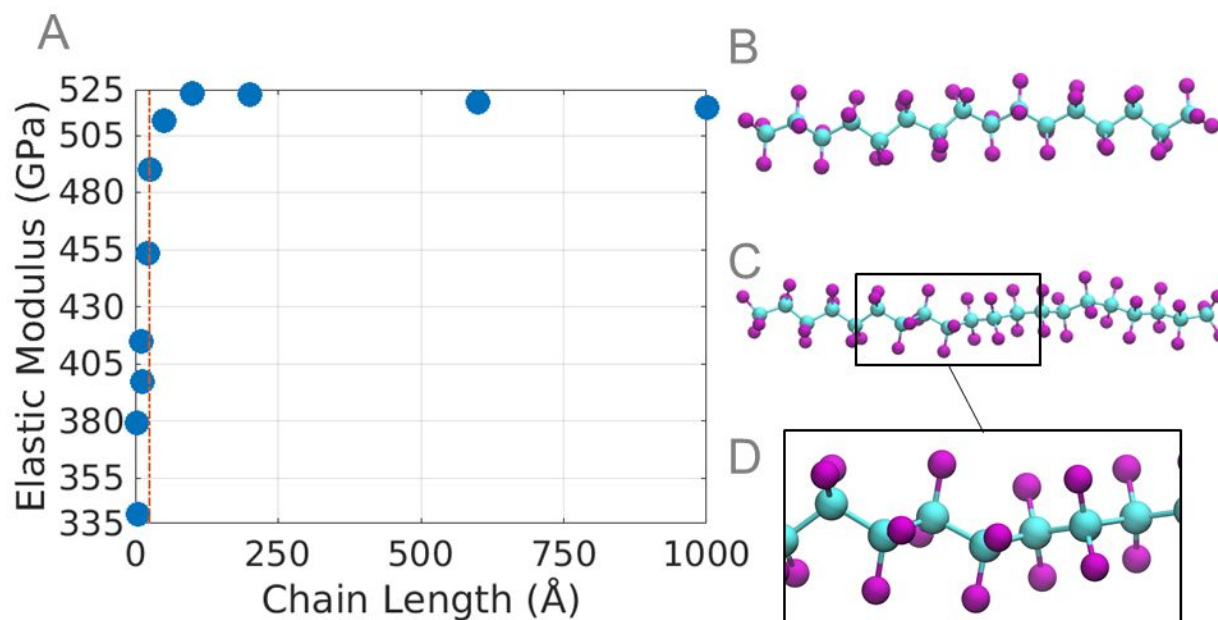


Figure 7 (A) Graph of elastic modulus vs chain length of PTFE at 300 K. The dotted line separates small chains ($< 25 \text{ \AA}$) from longer chains ($\geq 25 \text{ \AA}$). Once the chain length reaches 25 \AA , a twist in the backbone of the chain is observed at equilibrium. When under tensile load, the chain stretches by unraveling the twist, any chain that does not have a twist has a significantly lower elastic modulus. (B) 21.3 \AA long chain at equilibrium showing straight chain without a dihedral twist. (C) 25 \AA long chain at equilibrium showing a single dihedral twist. (D) Close up view of the twist in the 25 \AA long chain.

PTFE is known to have a torsion angle of approximately 162.5 degrees.^{52,53} At equilibrium, the carbon backbone of PTFE gradually rotates under the torsion angle, however, we observe at a length of 21.3 \AA (with 20 carbon atoms) a twist occurring in the chain. Chains with more than 20 carbon atoms all are observed to have at least one twist at equilibrium. During the tensile test dihedral angles slowly unravel, bond angles increase, and bond lengths stretch. Failure ultimately occurs when the bond between carbon atoms stretches too far. Chains with a twist are observed to have an extra phase where the twist is unraveled before bond lengths or bond angles increase. Once the twist has straightened, the dihedrals, bond angle, and bond lengths increase simultaneously just as observed in the chains without the twist. This explains the variation of modulus values.

3.1.2 The Effects of Initial Chain Length on Maximum Stress

When hydrated, the initial stress of the chain increases, as well as the maximum stress the chain can withstand. In every simulation, the chain with water surpasses the strength of the chain

without water. Nanoscale tensile tests in vacuum (figure 8A) show only a small change in maximum stress as chain length increases. Chain lengths investigated range from 25 Å to 1000 Å. The 25 and 50 Å chain lengths both in water and vacuum exhibit a slightly larger maximum stress than the longer chains. The increase in strength is due to the decreased initial stress in the shorter PTFE chains prior to the tensile test. To prevent the curling of the chains during equilibration, the ends of the chain are prevented from moving in any direction except the direction parallel to the chain orientation (X direction), leaving the chain in a state of stress visualized in figure 8C, and graphically by the non-zero stress at zero strain in figure 8A. The residual stress in the chains increase as the length of the chain increases, resulting in lower maximum stress values for the longer chains.

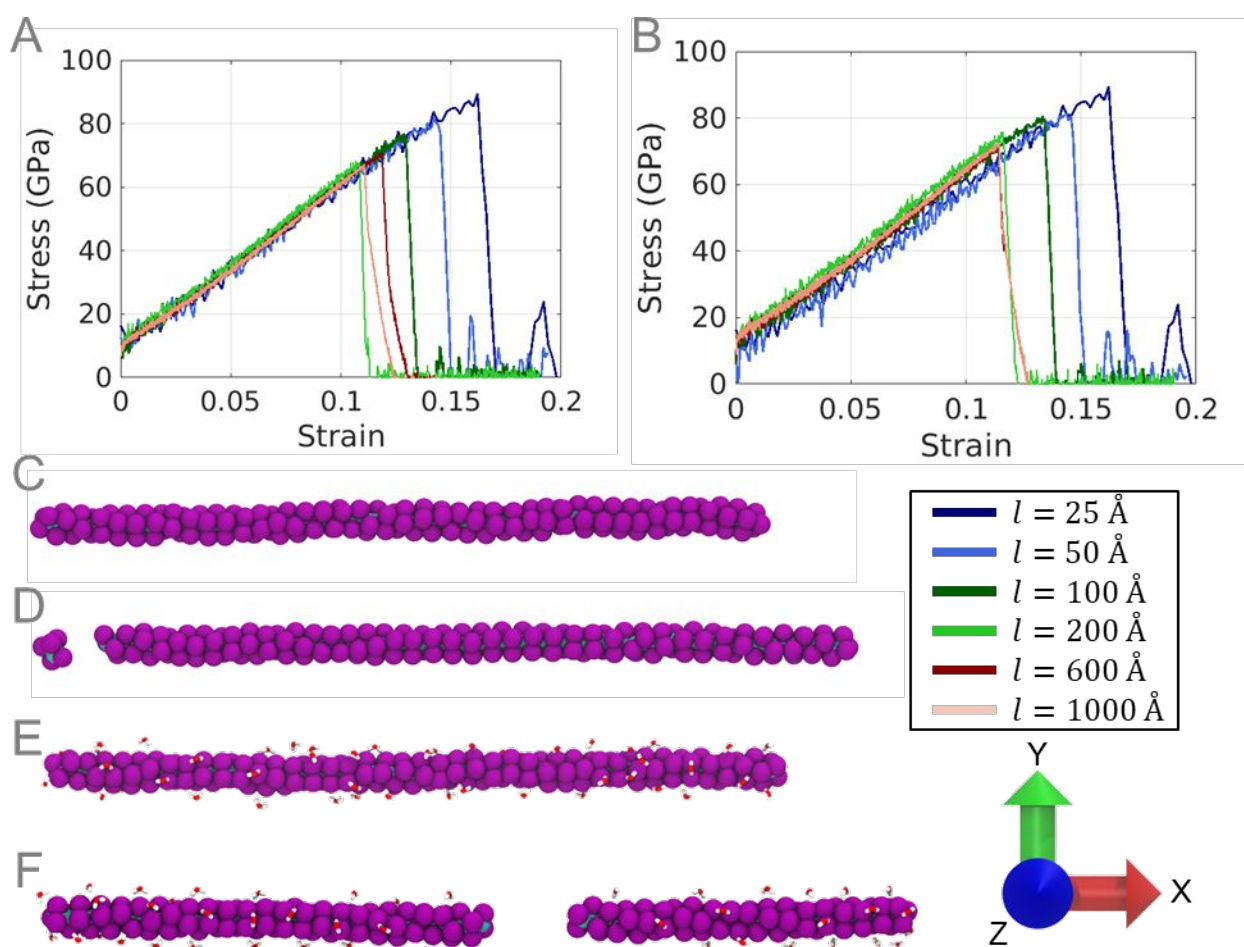


Figure 8 (A) Stress strain plot for PTFE in vacuum and (B) in water. (C) PTFE 100 Å long after equilibration and (D) after break. (E) PTFE 100 Å long in water environment after equilibration and (F) after break.

The maximum stress for longer chains decreases as the length of the chain increases, but appears to plateau at a length of 100 Å. A similar phenomenon was observed in polyynes where the smaller length chains were also reported to have a higher strength.^{54,55} The dependency the maximum strength of the chain has on length can be explained by the high axial strain energy for shorter chains, as well as the increase in probability that longer chains will break due to the increased number of bonds.

3.1.3 The Effect of Water and Vacuum Environments on Maximum Stress

The addition of water to the PTFE chains increases the maximum tensile stress before the chain breaks (figure 9A). The models which have been hydrated can withstand 4-8% more stress than their vacuum counterparts. Interestingly, the shorter chain lengths appear to benefit less from the water than the longer chain lengths. There was no covalent bonding, healing, or altering of the PTFE chain physical attributes during the simulations.

Water has been observed to increase the maximum strength of polyynes, but through a very different mechanism.⁵⁵ In PTFE, water is able to prevent the chain from excessive movement in the Y or Z directions. The chain with water, being hindered in two dimensions, is able to withstand a greater stress because the shape of the chain is more unified in the direction of the tensile load. An illustration of a chain under tensile load with water can be seen in figure 9B, the stabilizing effects are apparent when compared to the chain without water. While in both illustrations the calculated engineering strain is the same, the actual length between individual carbon bonds is greater in the chain without water, and therefore has a larger stress. This increase in bond distance is what ultimately causes the chain to fail.

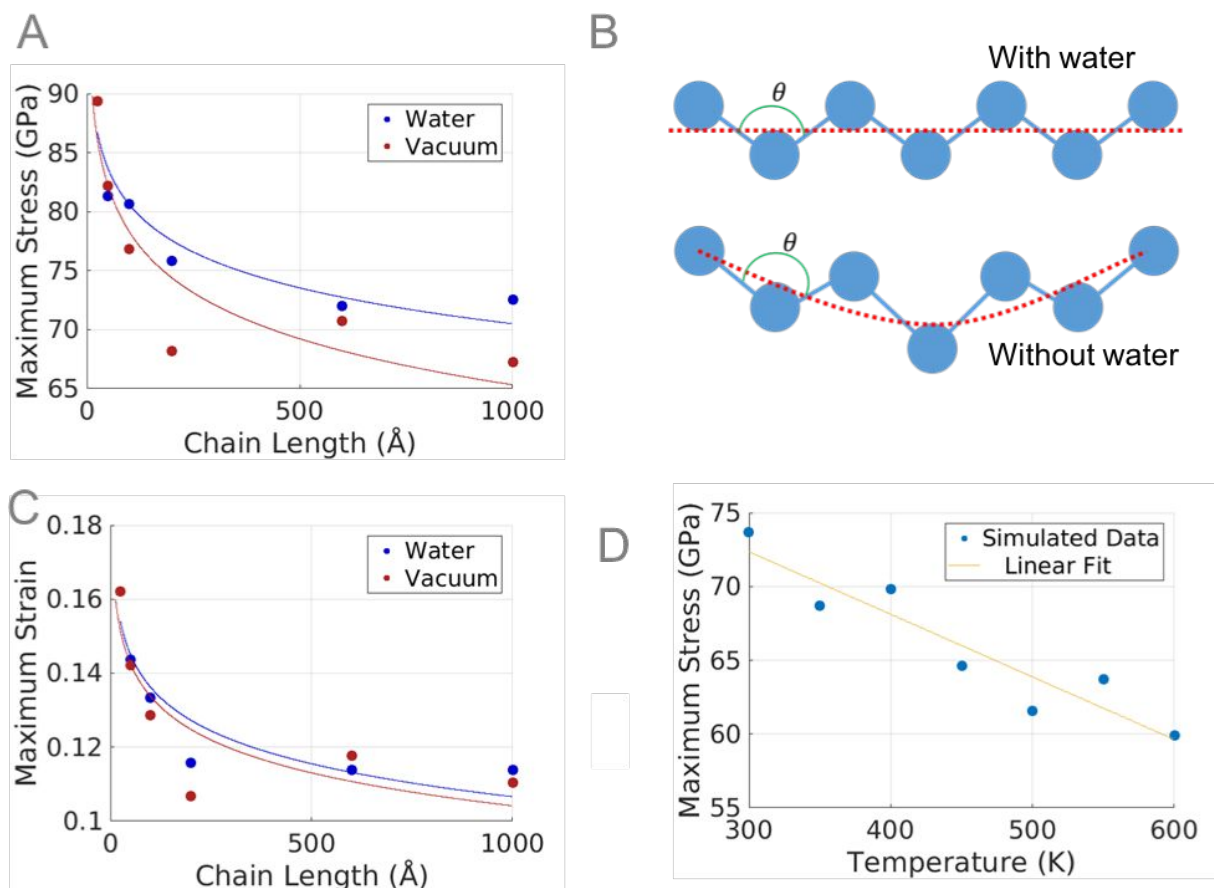


Figure 9 (A) Initial PTFE chain length vs maximum tensile stress before chain breaks, showing that the maximum tensile stress experienced by PTFE chains can be increased by adding water to stabilize the chain. It is observed that the maximum tensile stress is decreased as the length of the chain increases, but this effect diminishes as the chain length increases. (B) An illustration of a single PTFE chain under tensile stress with water. The water acts as a stabilizer and prevents redundant movements. Illustration of a PTFE chain without the water stabilizing effect. (C) Initial length of PTFE chain vs strain at break. The strain at break decreases as the length of the chain increases, but again plateaus similar to the max tensile stress. (D) Temperature of chain vs the maximum tensile stress. As temperature increases, we observe that the maximum stress of the PTFE chains decreases.

3.1.4 The Effect of Temperature Variation

We study the effect of temperature on PTFE chain by varying the temperature from 300 K to 600 K incrementing by 50 K and performing a tensile test. The temperature of the PTFE chain drastically affects the strength of the polymer (figure 9D). The maximum stress before the chain breaks has a negative correlation with the temperature of the chain. With the increase in kinetic

energy of the atoms, it becomes easier to break the bonds of the chain. Similar results have been recorded on macroscale PTFE in tension, the higher the temperature, the lower the yield stress.⁵⁶ During a scratch test on PTFE film, chains are observed to break and radicals are formed. With the increase in rubbing cycles, more chains are broken and radicals are formed.²³ It has been observed that higher temperatures cause a decrease in the coefficient of friction as well as a reduction in the adhesive forces between PTFE chains.³³ High temperatures that occur during rubbing of a PTFE film can be attributed with the failure of the film, and the increase of radicals.

3.1.5 Single Chain Study Summary

The shorter PTFE chains are observed to have up to 9% higher ultimate stress which decreases as the length of the chain increases. This decrease in strength is due to the high axial strain energy for longer chains, and the increased probability of a broken bond as the chains get longer. Water stabilizes the chains by limiting movement to the strain direction. PTFE chains exhibit lower strength as temperature raises from 300 K to 600 K. The calculated Young's Modulus for a 100 Å long PTFE chain at 300 K in vacuum is 525 GPa.

3.2 Nanoscale Indentation and Scratch Simulations

In order to predict the frictional properties, a bulk PTFE model is indented 10 Å by an indenter with a radius of 25 Å. After indentation, scratch tests are performed at three different scratch angles: 0 degrees, 45 degrees, and 90 degrees parallel to the chain orientation (Z axis).

3.2.1 Molecular Dynamics Indentation Results

The indentation force and the indentation depth are measured during this simulation (figure 10A). Under the compressive load, when the indentation force reach 400 nN (figure 10i) a chain is then displaced from the PTFE surface by the force of the indenter (figure 10ii). As the indenter continues through the PTFE, the indentation force continues to rise and more chains are displaced from the surface (figure 10iii).

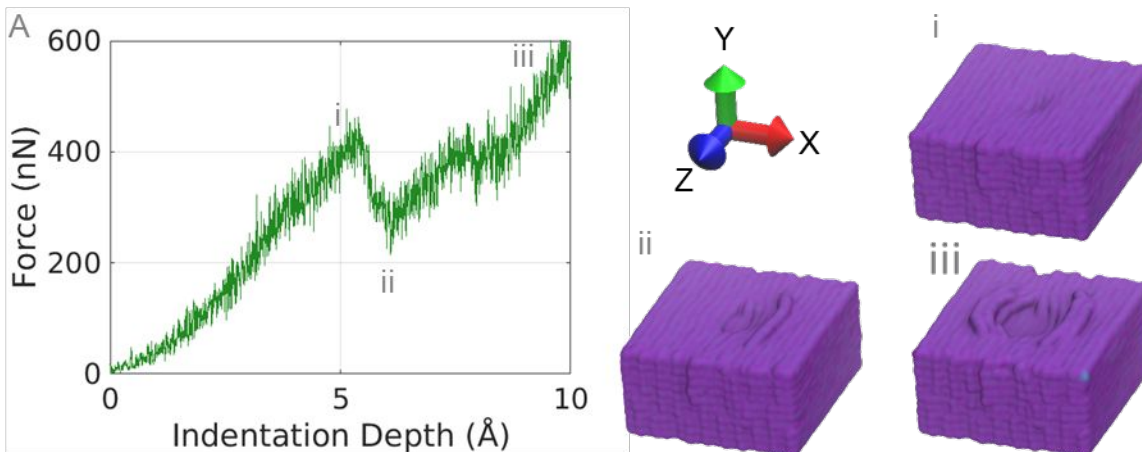


Figure 10 (A) Indentation Force vs Indentation Depth. Drops in the indentation force occur as chains are ejected from the surface of the PTFE. (i) Image of PTFE surface during indentation at the first peak in the force displacement plot before any chains are ejected. (ii) Image showing a PTFE chain protruding from the surface causing a drop in the force displacement plot. (iii) After 10 Å of indentation, multiple chains have been ejected from their original positions and are now protruding from the surface.

No chains are observed to break during indentation and the chain displacement phenomena occurred on both the first and second layers of PTFE. The maximum tensile stress a single chain of PTFE can withstand is approximately 80 GPa (figure 8A), we see the maximum force sustained by the bulk PTFE model is 400 nN before chains protrude from the surface of the PTFE. Dividing the maximum force before deformation by the approximate contact area of the indenter (πr^2), the contact pressure on the bulk PTFE is 20.37 GPa. The chains slip around the indenter at the same pressure as they would break under tensile stress. Because PTFE chains have an intrinsically low adhesion to each other, it is easy to separate the chains during indentation without significant damage to the PTFE surface.⁸ This allows for the chains to separate without breaking and to deform away from the indenter.

The elastic modulus of the bulk PTFE was found by computing stress by dividing the normal force by the contact area of the indenter, and a strain by computing the compressive strain on the center of the PTFE sample. The elastic modulus during indentation is 80.23 GPa for the first 5% strain. Experimental studies on thin film PTFE have been conducted investigating the thickness effect of PTFE on the elastic modulus, showing that decreasing film size greatly increases the elastic modulus of the film. While no direct comparison is available, the smallest PTFE film

tested by Wang et al had a thickness of 48.1 nm and an elastic modulus of 12 GPa, where our film thickness is 5.5 nm and has an elastic modulus of 80.23 GPa.⁵⁷

3.2.2 Nanoscale Scratch Test

Once an indentation depth of 10 Å is reached, a scratch test is performed on the surface for 10 Å. A scratch angle of 0 degrees (parallel to the chain orientation in the Z axis) shows a zipper like deformation during the scratch. The 0 degree scratch shows the ability of PTFE to deform without damaging the surface. The sections of chains in front of the indenter are displaced out of the indenter path, while the sections behind the indenter return to their original positions. This is because the PTFE chains have a relatively low adhesion force to one another. The van der Waals forces that attract the chains are easily separated by the indenter resulting in the parting of chains while the chains fall naturally back to their original positions due to the attraction forces from the neighboring chains.

A scratch angle of 90 degrees (perpendicular to the chain orientation) shows major deformation of the chains. Pile-up occurs (figure 10iii) as the indenter moves through the surface of the PTFE, and the chains behind the indenter remain relatively motionless. During the scratch test, the sections of chain in the path of the indenter cause pile-up. While the chains are forced out of their initial positions, the ends of the chains cannot remain connected to the neighboring chains. The ends of the chains slip past the neighboring fluorine atoms causing the drop in the force displacement graph (figure 11A), and coefficient of friction graph (figure 11B). The large drop occurring around 6 Å occurs when a chain is displaced from the surface of the PTFE, seen as the top chain in figure 11E.

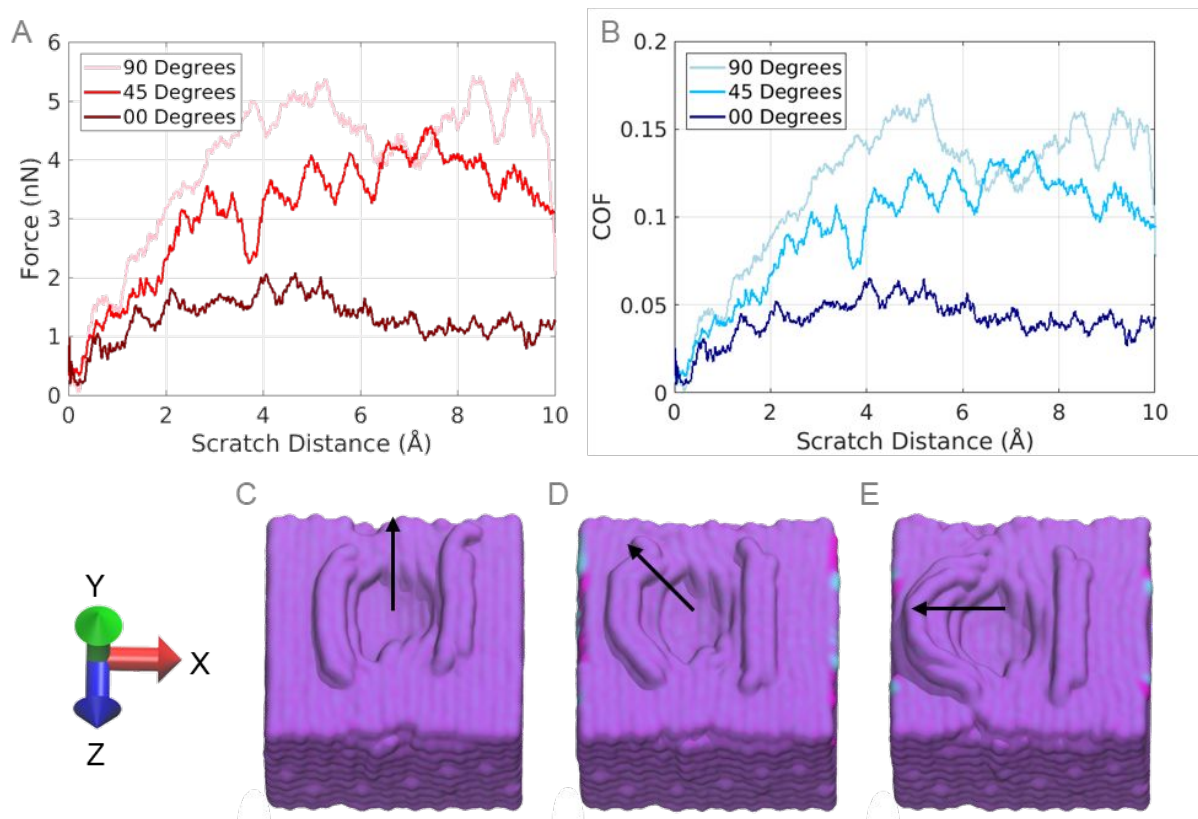


Figure 11 (A) Indentation force vs scratch distance for scratch angles of 0, 45, and 90 degrees. (B) Coefficient of friction computed from scratch tests at 0, 45, and 90 degree scratch angles. (C) Scratch distance of 10 Å for 0 degree scratch angle showing an arrow illustrating the scratch path. Chains have been displaced during the indentation but the scratch does not create more ejected chains. The indenter acts like a zipper, opening the PTFE surface by separating the individual chains. (D) Scratch distance of 10 Å for 45 degree scratch angle showing an arrow illustrating the scratch path. The chains ejected during the indentation are deformed slightly, but no new chains have been ejected from the surface. (E) Scratch distance of 10 Å for the 90 degree scratch angle. This image shows the pile-up of debris as the indenter displaces individual chains from the surface.

The results for scratch angle of 45 degrees shows a mixture between the 0 and 90 degree scratch angles. Chains in front of the indenter path have a low resistance to indentation and will deform to allow the indenter to pass over them, but are eventually displaced similar to the 90 degree scratch. Pile-up was not observed for the length of the scratch at 45 degrees. Similar to the 90 degree scratch, sudden decrease in the force displacement graphs are caused by the slipping of chains past neighboring chains. Unlike the 90 degree scratch angle, the chains are never displaced far enough to cause a chain to completely detach from the surface.

From the observations of these results, we can conclude that the polymer orientation during scratch is much less resistant when the chains are oriented in the same direction as the indenter direction. This result is supported by Barry et al who investigated sliding directions of PTFE sheets.³³ The PTFE sheets were observed to break and some chains reoriented based off of sliding direction. Frictional forces reported by Barry et al range from 2.1 to 10.7 nN, well within the values found in this work.³³

Coefficient of friction values for the 90 degree scratch average to 0.15. The 45 degree scratch shows values of 0.1 while the 0 degree scratch averages to 0.05. Previously reported values of the coefficient of friction for PTFE fall between 0.1 and 0.16 during initial sliding of PTFE.^{9,20} The coefficient of friction reported in this work support the values found in experimental work of bulk PTFE during the initial sliding of a scratch test. During scratch, experimental studies observe a decrease in the coefficient of friction, after the initial scratch has begun which may be result of chains reorienting to the scratch direction.¹⁰

3.2.3 Summary of MD Indentation and Scratch Studies

Indentation on PTFE shows some self-repairing characteristics due to the weak secondary bonds of PTFE chains. Chains begin to be ejected from the surface of the film at 400 nN of force. After 10 Å of indentation, multiple chains have been ejected from the PTFE film surface. Scratching parallel to chain orientation shows a COF of 0.05, scratching at a 45 degree angle to the chain orientation shows a COF of approximately 0.1, and the 90 degree scratch angle shows a COF of 0.15.

3.3 Coarse-grained Model Indentation and Scratch

We preform indentation and scratch studies on coarse-grained particles (flat, needle and porous) to predict their frictional properties. These are the common geometries of PTFE found at the microscale and can affect the frictional properties of PTFE coating.

3.3.1 Indentation of Coarse-grained PTFE Particles

During indentation of the coarse-grained particles (figure 12A), the porous particle required the least force for the indenter to penetrate the particle. Because of the low density of the particle, most of the indentation depth is used to compress the fibers the indenter encounters. The porous particle compacts, and shears slightly in the positive Z direction, which is most likely due to the internal structure of the particle. The inside structure of the particle has column like supports

created from high density tangled fibers, oriented in random directions. The largest support near the indenter extends in the positive Z direction, so when it is compressed, the support causes shear in the entire particle in the Z direction.

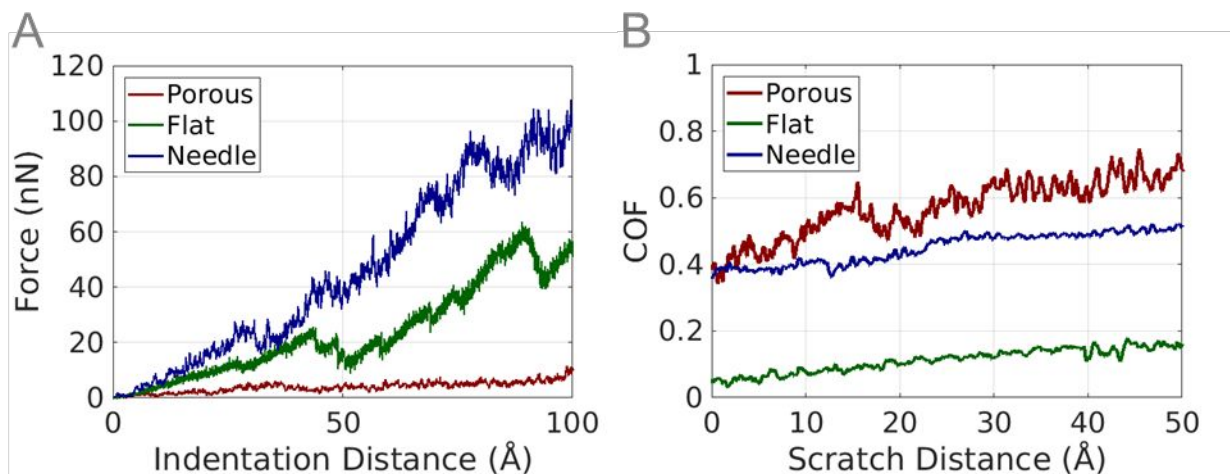


Figure 12 A) Plot of indentation distance vs indentation force showing the denser a particle is, the greater the force is needed to indent the same indentation depth. B) Coefficient of friction during the scratch in the X direction. The flat particle has a low initial coefficient of friction value which increases due to increasing resistance from the shearing surface. Since the surface of all particles is uneven, the indenter experiences increasing or decreasing frictional forces depending on the amount of material obstructing the indentation motion.

The flat particle shows a much greater resistance to the indenter than the porous particle. As the indenter begins to penetrate the surface of the flat particle, the compression of the fibers begins immediately. Due to the high density, the fibers cannot compress much farther and the force begins to rise. Sudden drops in the force displacement graph occur when support columns or groups of fibers slip past other support columns or fibers. The flattened particle undergoes a shearing similar to the porous model, unlike the porous particle, most of the flat particle support columns are oriented horizontally due to the compression used to create the flat surface. The lower half of the particle is more porous than the top half, and is mainly responsible for the shear visible in the particle during the scratch.

The force measured during the indentation of the needle particle was larger in magnitude than the force measured on any of the other particles. The indenter contacts the particle surface on top of a raised segment of the particle. Drops in the force displacement plot again correspond to

slipping of support columns past other columns in the model (figure 2F). Because the density of the needle particle is slightly higher than the flat particle, the drops in force are not high, as the support columns have less space to slip into.

3.3.2 Scratch Test of Coarse-grained Models

Scratch test on the porous particle had little resistance to the indenter (figure 12B), similar to the results from the indentation studies. As the indenter scratches the surface of the porous particle the indenter remains at the initial indentation depth of 100 Å. The frictional coefficient gradually increases throughout the simulation due to the slope of the surface topography, and continually shearing PTFE fibers, which is seen during the scratch test of all particles. While the normal and frictional forces measured during the scratch test are low, the coefficient of friction is high due to the large amount of resistance from the topography of the particle. The density of summits (S_{ds}) of the particle is calculated by counting the peaks and dividing by the surface area of the particle (figure 13A), the density of summits of the porous particle is $2.242 \times 10^{-3} \text{ nm}^{-2}$.⁵⁸ The deviation of summit heights (S_{dv}) is also calculated (figure 13B) and the porous particle has a summit height deviation of 31.56 nm.

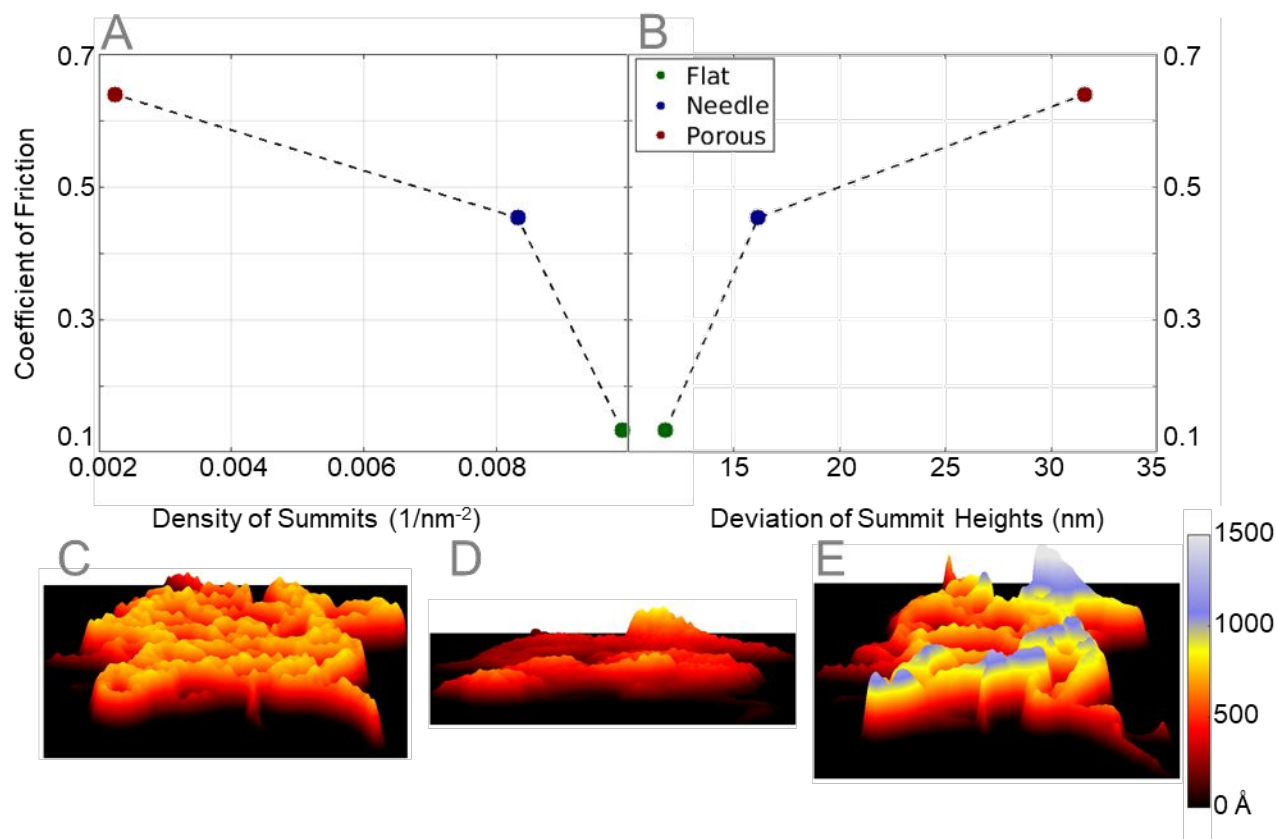


Figure 13 A) Density of summits vs coefficient of friction showing the higher the density of summits on the particle, the lower the coefficient of friction. B) Deviation of summit heights vs coefficient of friction showing the lower the deviation the lower the coefficient of friction. C) Flat particle surface topography which has more peaks at a constant height. D) Needle particle surface topography showing a few peaks at varying heights. E) Porous particle showing greatest peak height and peak height variation.

The coefficient of friction of the flat particle steadily increases from 0.03 to 0.20 (figure 12B). Small fluctuations in the coefficient of friction are seen at 40 Å scratch distance which are caused by shear deformation in the particle. Three more scratch tests were performed at 10 Å intervals where coefficient of friction values ranged from 0.05 to 0.2. The additional scratch tests provide evidence that the coefficient of friction varies depending on the surface topography. The density of summits for the flat particle is $9.903 \times 10^{-3} \text{ nm}^{-2}$ and the deviation of summit heights is 11.17 nm. The flat particle has the highest density of summits and the lowest deviation of summit heights. These localized peaks help reduce friction, as less material is able to come in contact with the indenter during the scratch test.

The needle particle has a high coefficient of friction similar to the porous particle. Three additional scratch tests were performed at 10 Å intervals. Coefficient of friction values ranged from 0.35 to 0.5 during the additional scratch tests. The density of summits for the needle particle is $8.325 \times 10^{-5} \text{nm}^{-2}$ and deviation of summit height of 16.16 nm.

The coefficient of friction calculated and plotted in figure 12B is calculated by running one scratch down the center of the particles. To estimate an error of these values, three more tests were performed on the flat and needle particles, scratching horizontal to the first scratch at intervals of 10 Å. The average coefficient of friction for the flat, needle, and porous particles are 0.1324, 0.4351, and 0.6392 respectively. Reported coefficient of friction values for PTFE film during micrometer length scratch tests range from 0.15 to 0.20 which are slightly higher than the coefficient of friction values for the flattened particle.⁵⁹ The attributes of the particles that govern the coefficient of friction values are the density of summits, and the deviation of summit heights. As seen in figure 13A, the higher the density of summits, the lower the coefficient of friction. The summit deviation also plays a big role in lowering the coefficient of friction (figure 13B), as the deviation of summit height decreases, the coefficient of friction also decreases.

The porous particle had the lowest summit density and highest deviation of summit height. The porous particle is modeled after the spherical particles seen before annealing a PTFE film. The porous particle takes a rather spherical shape, which allows the PTFE fibers to stay as straight as possible and bend the least number of times. The needle particle has a much higher density than the porous particle, causing the PTFE fibers to bend to fit more particles in a smaller area. The bending and buckling of fibers cause an increase in summit density, and a decrease in the deviation of summit height. The compression of the porous particle increases the density of summits by forcing the relatively straight PTFE fibers to form a dense straight edge on the surface of the flat particle. This dense edge of the flat particle is compressed to the same height therefore decreasing the deviation of summit heights.

3.3.3 Summary of coarse-grained simulations

A coarse-grained model is obtained from the results of fully atomistic molecular dynamics simulations which allows for the investigation of much larger length scales. Equilibration of the coarse-grained models show that PTFE chains would prefer to remain straight, but due to the sheer number and length of chains, will form an amorphous particle. Indentation on porous, flat,

and needle shaped particles show that the particles with higher density will require a higher force to indent. Scratch tests reveal that a particle with higher summit density and lower deviation of summit height will have a lower coefficient of friction. Coefficient of friction values of the coarse-grained particles fall within the values calculated during the MD simulations, and the coefficient of friction value for the flattened particle agrees with experimental studies.

4 Conclusions

We have investigated single PTFE chain strength and found that the length of the chain does not affect the strength of the PTFE chain except for very short chains. Adding water strengthens the PTFE chain, while the pulling rate does not affect the maximum stress of the chain. Increasing the temperature of the chain decreases the tensile strength of the PTFE chain.

We also studied nanoindentation of compact PTFE on the nanoscale using molecular dynamics. We observed that PTFE chains slip around the indenter after 5 Å of indentation depth, which is equal to the depth of one layer of PTFE chains, or 400 nN of force. PTFE chains resisted scratch much greater when the scratch direction was perpendicular to the chain orientation resulting in deformation of the PTFE surface.

We generated a bundle of PTFE chains to derive the coarse-grained potential for microscale PTFE. Three different particle shapes were investigated, the porous, flattened, and the needle, modeled after experimental observations of PTFE particles. We observed that PTFE tends to form relatively straight fibers which gather to create a porous interwoven mesh. The maximum strength of PTFE particles tested using the coarse-grained force field was 60 nN before severe deformation occurred, approximately 6 times weaker than results of PTFE on the nanoscale using the ReaxFF force field.

Indentation on the porous nanoparticle using the coarse-grained model showed least resistance to indentation, while the flattened particle showed a greater resistance, and the needle particle showed the greatest resistance to indentation. Each model had slightly greater density than the last, suggesting the greater the density of the particle the more resistant to indentation the particle will be. The deformation of each of these particles was similar, showing that the deformation of an individual particle is based on the internal structure of the particle, not just the surface topography or the shape.

Scratch tests performed on the three micrometer sized particles show how the surface topography, shape, and density of a particle will affect the coefficient of friction. The value of the coefficient of friction is affected mainly by the density and height deviation of peaks in the particle. The coefficient of friction is highest when the particle has a low density of summits, and a high deviation of summit height. The coefficient of friction values for the coarse-grained models ranged from 0.13 to 0.64 while reported values for experimental coefficient of friction values range from 0.1 to 0.3^{7,8,21} and accepted numerical simulations at the nanoscale range from 0.1 to 0.6.^{4,33}

The generation of the coarse-grained model and potential allows for the modeling of PTFE on a microscale reaching length scales that have not previously been possible. The results from indentation and scratch tests performed on the coarse-grained PTFE model show that high density and even surface roughness create the PTFE particle with the lowest coefficient of friction. Further investigations of micrometer sized PTFE particles can illuminate phenomena seen in PTFE thin films, such as adhesion mechanisms, interaction with filler particles, and the effects of fiber length, thus paving the path for modeling of more realistic PTFE surfaces. The studies outlined here will enhance the possibilities of PTFE for multi-disciplinary applications.

5 Conflicts of Interest

There are no conflicts to declare.

6 Acknowledgements

We sincerely thank the Center for Advanced Surface Engineering, under the National Science Foundation Grant No. OIA-1457888 and the Arkansas EPSCoR Program, ASSET III, Funding for this research. Authors would like to acknowledge the support in part by the National Science Foundation under the grants ARI#0963249, MRI#0959124 and EPS#0918970, and a grant from Arkansas Science and Technology Authority, managed by Arkansas High Performance Computing Center.

- (1) Sui, H.; Pohl, H.; Schomburg, U.; Upper, G.; Heine, S. Wear and friction of PTFE seals. *Wear* **1999**, *224*, 175-182.
- (2) Klinkert, P.; Post, P.; Breslau, P.; Van Bockel, J. Saphenous vein versus PTFE for above-knee femoropopliteal bypass. A review of the literature. *European Journal of Vascular and Endovascular Surgery* **2004**, *27*, 357-362.
- (3) Burris, D. L.; Sawyer, W. G. Tribological sensitivity of PTFE/alumina nanocomposites to a range of traditional surface finishes. *Tribology Transactions* **2005**, *48*, 147-153.
- (4) Harris, K. L.; Pitenis, A. A.; Sawyer, W. G.; Krick, B. A.; Blackman, G. S.; Kasprzak, D. J.; Junk, C. P. PTFE tribology and the role of mechanochemistry in the development of protective surface films. *Macromolecules* **2015**, *48*, 3739-3745.
- (5) DEBIES, L. M. T.; TAKACS, G. Adhesion of copper to poly (tetrafluoroethylene) surfaces modified with vacuum UV radiation downstream from He and Ar microwave plasmas. *Polymer Surface Modification: Relevance to Adhesion* **2004**, *3*, 139.
- (6) Plunkett, R. J. In *Tilte*1986; Springer.
- (7) Flom, D.; Porile, N. Friction of teflon sliding on teflon. *Journal of Applied Physics* **1955**, *26*, 1088-1092.
- (8) King, R.; Tabor, D. The effect of temperature on the mechanical properties and the friction of plastics. *Proceedings of the Physical Society. Section B* **1953**, *66*, 728.
- (9) Makinson, K. R.; Tabor, D. In *Tilte*1964; The Royal Society.
- (10) Beckford, S.; Mathurin, L.; Chen, J.; Fleming, R. A.; Zou, M. The effects of polydopamine coated Cu nanoparticles on the tribological properties of polydopamine/PTFE coatings. *Tribology International* **2016**, *103*, 87-94.
- (11) Liu, X.-X.; Li, T.-S.; Liu, X.-J.; Lv, R.-G.; Cong, P.-H. An investigation on the friction of oriented polytetrafluoroethylene (PTFE). *Wear* **2007**, *262*, 1414-1418.
- (12) Blanchet, T.; Kennedy, F. Sliding wear mechanism of polytetrafluoroethylene (PTFE) and PTFE composites. *Wear* **1992**, *153*, 229-243.
- (13) Deli, G.; Qunji, X.; Hongli, W. Study of the wear of filled polytetrafluoroethylene. *Wear* **1989**, *134*, 283-295.
- (14) Conte, M.; Pinedo, B.; Igartua, A. Role of crystallinity on wear behavior of PTFE composites. *Wear* **2013**, *307*, 81-86.
- (15) Lai, S.-Q.; Yue, L.; Li, T.-S.; Hu, Z.-M. The friction and wear properties of polytetrafluoroethylene filled with ultrafine diamond. *Wear* **2006**, *260*, 462-468.
- (16) Blanchet, T.; Kennedy, F.; Jayne, D. XPS analysis of the effect of fillers on PTFE transfer film development in sliding contacts. *Tribology transactions* **1993**, *36*, 535-544.
- (17) De-Li, G.; Bing, Z.; Qun-Ji, X.; Hong-Li, W. Effect of tribochemical reaction of polytetrafluoroethylene transferred film with substrates on its wear behaviour. *Wear* **1990**, *137*, 267-273.
- (18) Tanaka, K.; Uchiyama, Y.; Toyooka, S. The mechanism of wear of polytetrafluoroethylene. *Wear* **1973**, *23*, 153-172.
- (19) Burris, D. L. Effects of nanoparticles on the wear resistance of polytetrafluoroethylene. University of Florida, 2007.
- (20) Burris, D. L.; Sawyer, W. G. Improved wear resistance in alumina-PTFE nanocomposites with irregular shaped nanoparticles. *Wear* **2006**, *260*, 915-918.
- (21) Shi, Y.; Feng, X.; Wang, H.; Liu, C.; Lu, X. Effects of filler crystal structure and shape on the tribological properties of PTFE composites. *Tribology International* **2007**, *40*, 1195-1203.
- (22) Beckford, S.; Mathurin, L.; Chen, J.; Zou, M. The influence of Cu nanoparticles on the tribological properties of polydopamine/PTFE+ Cu films. *Tribology Letters* **2015**, *59*, 11.
- (23) Beckford, S.; Zou, M. Wear resistant PTFE thin film enabled by a polydopamine adhesive layer. *Applied Surface Science* **2014**, *292*, 350-356.
- (24) Sawyer, W. G.; Freudenberg, K. D.; Bhimaraj, P.; Schadler, L. S. A study on the friction and wear behavior of PTFE filled with alumina nanoparticles. *Wear* **2003**, *254*, 573-580.

- (25) Pitenis, A. A.; Harris, K. L.; Junk, C. P.; Blackman, G. S.; Sawyer, W. G.; Krick, B. A. Ultralow wear PTFE and alumina composites: it is all about tribochemistry. *Tribology Letters* **2015**, *57*, 4.
- (26) Ye, J.; Khare, H.; Burris, D. Quantitative characterization of solid lubricant transfer film quality. *Wear* **2014**, *316*, 133-143.
- (27) Blanchet, T. A.; Kandanur, S. S.; Schadler, L. S. Coupled effect of filler content and countersurface roughness on PTFE nanocomposite wear resistance. *Tribology Letters* **2010**, *40*, 11-21.
- (28) Aderikha, V.; Krasnov, A.; Shapovalov, V.; Golub, A. Peculiarities of tribological behavior of low-filled composites based on polytetrafluoroethylene (PTFE) and molybdenum disulfide. *Wear* **2014**, *320*, 135-142.
- (29) Jintang, G.; Hongxin, D. Molecule structure variations in friction of stainless steel/PTFE and its composite. *Journal of applied polymer science* **1988**, *36*, 73-85.
- (30) Krick, B. A.; Ewin, J. J.; Blackman, G. S.; Junk, C. P.; Sawyer, W. G. Environmental dependence of ultra-low wear behavior of polytetrafluoroethylene (PTFE) and alumina composites suggests tribochemical mechanisms. *Tribology International* **2012**, *51*, 42-46.
- (31) Chen, S.; Wang, J.; Ma, T.; Chen, D. Molecular dynamics simulations of wetting behavior of water droplets on polytetrafluoroethylene surfaces. *The Journal of chemical physics* **2014**, *140*, 114704.
- (32) Heo, S. J.; Jang, I.; Barry, P. R.; Phillpot, S. R.; Perry, S. S.; Sawyer, W. G.; Sinnott, S. B. Effect of the sliding orientation on the tribological properties of polyethylene in molecular dynamics simulations. *Journal of Applied Physics* **2008**, *103*, 083502.
- (33) Barry, P. R.; Chiu, P. Y.; Perry, S. S.; Sawyer, W. G.; Sinnott, S. B.; Phillpot, S. R. Effect of temperature on the friction and wear of PTFE by atomic-level simulation. *Tribology Letters* **2015**, *58*, 50.
- (34) Herbold, E.; Cai, J.; Benson, D.; Nesterenko, V. In *Tilte2007*; AIP.
- (35) Elliott, J. A.; Wu, D.; Paddison, S. J.; Moore, R. B. A unified morphological description of Nafion membranes from SAXS and mesoscale simulations. *Soft Matter* **2011**, *7*, 6820-6827.
- (36) Wescott, J. T.; Qi, Y.; Subramanian, L.; Weston Capehart, T. Mesoscale simulation of morphology in hydrated perfluorosulfonic acid membranes. *The Journal of chemical physics* **2006**, *124*, 134702.
- (37) Wu, D.; Paddison, S. J.; Elliott, J. A.; Hamrock, S. J. Mesoscale modeling of hydrated morphologies of 3M perfluorosulfonic acid-based fuel cell electrolytes. *Langmuir* **2010**, *26*, 14308-14315.
- (38) Buehler, M. J. Mesoscale modeling of mechanics of carbon nanotubes: self-assembly, self-folding, and fracture. *Journal of materials research* **2006**, *21*, 2855-2869.
- (39) Mirzaeifar, R.; Qin, Z.; Buehler, M. J. Mesoscale mechanics of twisting carbon nanotube yarns. *Nanoscale* **2015**, *7*, 5435-5445.
- (40) Van Duin, A. C.; Dasgupta, S.; Lorant, F.; Goddard, W. A. ReaxFF: a reactive force field for hydrocarbons. *The Journal of Physical Chemistry A* **2001**, *105*, 9396-9409.
- (41) Singh, S. K.; Srinivasan, S. G.; Neek-Amal, M.; Costamagna, S.; van Duin, A. C.; Peeters, F. Thermal properties of fluorinated graphene. *Physical Review B* **2013**, *87*, 104114.
- (42) Plimpton, S.; Crozier, P.; Thompson, A. LAMMPS-large-scale atomic/molecular massively parallel simulator. *Sandia National Laboratories* **2007**, *18*.
- (43) Humphrey, W.; Dalke, A.; Schulten, K. VMD: visual molecular dynamics. *Journal of molecular graphics* **1996**, *14*, 33-38.
- (44) Gill, F. S.; Chandra, S.; Panwar, V.; Uniyal, D.; Kalra, G.; Kumar, V.; Garg, P. Conduction pathways in CNF/PTFE composite: Air oxidized CNFs coated with the incomplete layer of PTFE. *Diamond and Related Materials* **2018**, *89*, 227-238.
- (45) Inayoshi, M.; Hori, M.; Goto, T.; Hiramatsu, M.; Nawata, M.; Hattori, S. Formation of polytetrafluoroethylene thin films by using CO₂ laser evaporation and XeCl laser ablation. *Journal of Vacuum Science & Technology A: Vacuum, Surfaces, and Films* **1996**, *14*, 1981-1985.

- (46) Xiong, S.; Kong, L.; Zhong, Z.; Wang, Y. Dye adsorption on zinc oxide nanoparticles atomic-layer-deposited on polytetrafluoroethylene membranes. *AIChE Journal* **2016**, *62*, 3982-3991.
- (47) Weidner, V. R.; Hsia, J. J. Reflection properties of pressed polytetrafluoroethylene powder. *JOSA* **1981**, *71*, 856-861.
- (48) Burris, D. L.; Sawyer, W. G. A low friction and ultra low wear rate PEEK/PTFE composite. *Wear* **2006**, *261*, 410-418.
- (49) Shimanouchi, T.; Asahina, M.; Enomoto, S. Elastic moduli of oriented polymers. I. The simple helix, polyethylene, polytetrafluoroethylene, and a general formula. *Journal of Polymer Science* **1962**, *59*, 93-100.
- (50) Bartha, F.; Bogar, F.; Peeters, A.; Van Alsenoy, C.; Van Doren, V. Density-functional calculations of the elastic properties of some polymer chains. *Physical Review B* **2000**, *62*, 10142.
- (51) Zhang, M.-L.; Miao, M.; Peeters, A.; Van Alsenoy, C.; Ladik, J.; Van Doren, V. LDA calculations of the Young's moduli of polyethylene and six polyfluoroethylenes. *Solid state communications* **2000**, *116*, 339-343.
- (52) D'Amore, M.; Talarico, G.; Barone, V. Periodic and high-temperature disordered conformations of polytetrafluoroethylene chains: an ab initio modeling. *Journal of the American Chemical Society* **2006**, *128*, 1099-1108.
- (53) Holt, D.; Farmer, B. Modeling of helix reversal defects in polytetrafluoroethylene: I. Force field development and molecular mechanics calculations. *Polymer* **1999**, *40*, 4667-4672.
- (54) Nair, A.; Cranford, S.; Buehler, M. The minimal nanowire: Mechanical properties of carbyne. *EPL (Europhysics Letters)* **2011**, *95*, 16002.
- (55) Mirzaeifar, R.; Qin, Z.; Buehler, M. J. Tensile strength of carbyne chains in varied chemical environments and structural lengths. *Nanotechnology* **2014**, *25*, 371001.
- (56) Rae, P.; Brown, E. The properties of poly (tetrafluoroethylene)(PTFE) in tension. *Polymer* **2005**, *46*, 8128-8140.
- (57) Wang, J.; Shi, F.; Nieh, T.; Zhao, B.; Brongo, M.; Qu, S.; Rosenmayer, T. Thickness dependence of elastic modulus and hardness of on-wafer low-k ultrathin polytetrafluoroethylene films. *Scripta materialia* **2000**, *42*.
- (58) Bhushan, B.: *Introduction to tribology*; John Wiley & Sons, 2013.
- (59) Unal, H.; Mimaroglu, A.; Kadioglu, U.; Ekiz, H. Sliding friction and wear behaviour of polytetrafluoroethylene and its composites under dry conditions. *Materials & Design* **2004**, *25*, 239-245.